Influence of Design Features on Underwater Towed System Stability

N. E. JEFFREY*
Defence Research Establishment Atlantic, Dartmouth, Nova Scotia, Canada

Development of faired cables has increased the feasible speed and depth of underwater towed systems, but a much more refined approach is now needed to obtain good dynamic stability with passively stabilized systems. Parametric analytical stability studies have demonstrated some fundamental effects of cable and body designs and their interactions on body behavior. These studies were based on a relatively simple mathematical model, which included approximate cable configuration parameters and body virtual masses and inertias. Results demonstate the existence of a mode dominated by cable configuration, a mode dependent on cable-body coupling effects, a mode primarily affected by body design and three modes unlikely to be of practical importance. Relative effects of primary cable and body design features are shown in root-locus form, and conclusions are drawn concerning their significance to the over-all system.

Nomenclature

m	=	towed body mass
$m_{x,\,y,\,z}$	=	total body mass, including virtual mass, in X, Y, or Z axis directions
$x,\ y,\ z$	=	body axis displacement disturbance
$x_G,\ z_G$	=	body center of gravity coordinates relative to towpoint axis origin
$x_0,\ z_0$	=	body distance aft and depth relative to cable intersection with water surface
$I_{x,\,y,\,z}$	=	total body inertia, including virtual inertia, about X, Y, and Z axes
I_{xz}	=	body product of inertia in x-z plane
$K,\ M,\ N$	=	applied rolling, pitching, and yawing moments about body axes
D	=	cable drag/ft
U_0	=	steady-state towing speed
$X,\ Y,\ Z$	=	applied forces along body axes
$\theta,\ \varphi,\ \psi$	=	pitch, roll and yaw angular disturbances
ω_n	=	undamped natural frequency
ω_d	=	damped natural frequency
ζ	=	damping ratio
$\dot{x}$, etc.	=	first derivative of x displacement with respect to time
X_x, etc.	=	rate of change of X force with x displacement evaluated at steady state (dimensional stability derivatives)

Introduction

THERE are many applications for underwater towed systems in oceanography, fishing, and maritime warfare, but there is a dearth of useful design information. Design of suitably stable systems has often proceeded with little more than rule of thumb guidelines. The recent development of faired towing cables has opened up new possibilities of higher speeds and depths, which call for a refined design approach.

The behavior of underwater towed systems is heavily dependent on the configuration assumed by the cable. Under steady-state, this configuration can be calculated by simple methods, recently summarized by Eames,[1] and designing to attain specified steady-state performance is straightforward. However, under dynamic conditions, there is little information of general guidance to the designer although several studies have been made.[2–7]

Presented as Paper 68-124 at the AIAA 6th Aerospace Sciences Meeting, New York, January 22–24, 1968; submitted February 5, 1968; revision received July 8, 1968.

* Scientific Officer, Fluid Mechanics Section. Member AIAA.

This paper presents results of a parametric study, based on a simple linear mathematical model, of the influence of basic body and cable design features on the dynamic stability of a passively stabilized system. Results are presented in root-locus form for each of the six modes of rigid body motion. Trends of three of these modes which are important in system design are highlighted. Although based on a particular parent body, the trends give useful guidance in system design.

Mathematical Model

Figure 1 shows the right handed, orthogonal body axis system with origin at the body towpoint, used to define rigid body kinematics. For simplicity, analysis is confined to small disturbances about an initial steady-state condition and to a rigid body symmetrical about its vertical centerline plane and with its center of gravity vertically below its towpoint. Under these assumptions, the longitudinal and lateral motions are uncoupled and may be represented by two independent sets of three equations as follows:

Longitudinal symmetric motion

$$m(\ddot{x} + z_G\ddot{\theta}) = \Sigma X \tag{1}$$

$$m(\ddot{z} - U_0\dot{\theta}) = \Sigma Z \tag{2}$$

$$mz_G\ddot{x} + I_y\ddot{\theta} = \Sigma M \tag{3}$$

Lateral antisymmetric motion

$$m(\ddot{y} + U_0\dot{\psi}) - mz_G\ddot{\varphi} = \Sigma Y \tag{4}$$

$$-mz_G(\ddot{y} + U_0\dot{\psi}) + I_x\ddot{\varphi} - I_{zx}\ddot{\psi} = \Sigma K \tag{5}$$

$$I_z\ddot{\psi} - I_{zx}\ddot{\varphi} = \Sigma N \tag{6}$$

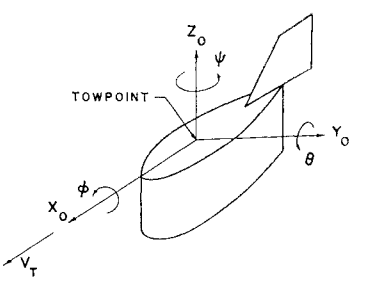

Fig. 1 Body axis system.

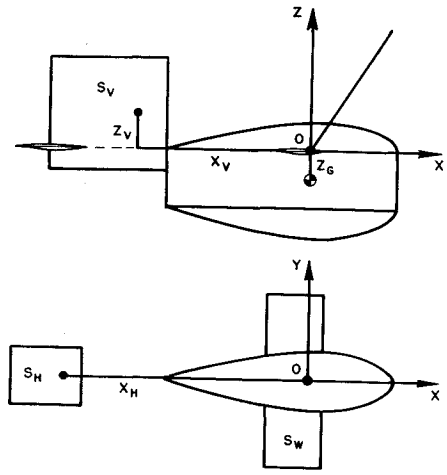

Fig. 2 Parent depressed body.

External forces and moments at the body towpoint arise from three primary sources: 1) added hydrodynamic mass and inertia, 2) body hydrodynamic effects, and 3) tow cable effects.

Inclusion of towing cable forces is the only major departure from aircraft stability analysis. The cable is a very complex system. Methods of analysis have ranged from direct integration techniques over a continuous cable, in some simple cases, to digital treatment of multisegment lumped masses using large, high-speed computers. However, there is experimental evidence[5,6] that the first-order mode of cable oscillation dominates its dynamic behavior.

Eames has developed approximate expressions for cable forces resulting from body displacement and velocity disturbances in surge heave and sway in the forms

$$\frac{\partial X}{\partial x} = -\frac{Rz_0}{2x_0} \qquad \frac{\partial X}{\partial \dot{x}} = -\frac{Rz_0}{U_0} \tag{7}$$

$$\frac{\partial Y}{\partial y} = -\frac{Rz_0}{2x_0} \qquad \frac{\partial Y}{\partial \dot{y}} = -\frac{Rz_0}{2U_0} \tag{8}$$

$$\frac{\partial Z}{\partial z} = -\frac{Rz_0}{x_0} \qquad \frac{\partial Z}{\partial \dot{z}} = -\frac{Rz_0}{2U_0} \tag{9}$$

A physical interpretation of these "cable derivatives" can be obtained by replacing the cable by imaginary mechanical springs and dampers along the axes. Displacement derivatives are the stiffnesses of these springs and velocity derivatives are corresponding damping factors.

The preceding equations are derived for a cable that is vertical at the body. In other cases, they are the forces tangential and normal to the cable, and resolved along the body axes.

The cable derivatives may be treated as conventional aerodynamic stability derivatives and the over-all mathematical

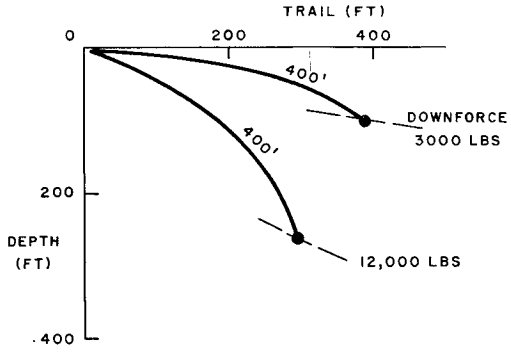

Fig. 3 Cable configurations at 40 knots.

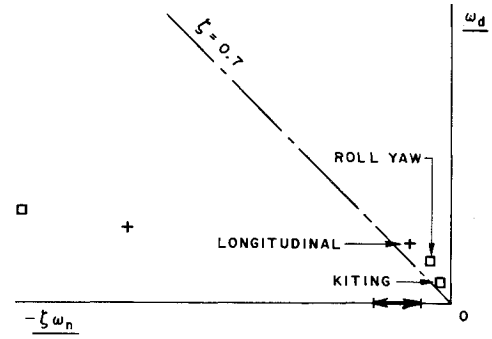

Fig. 4 Parent depressed system characteristics.

model thus becomes two independent sets of three linear differential equations with constant coefficients. The solution of each set leads to a characteristic sixth-order polynomial, which may contain up to three pairs of complex conjugate roots defining three modes of motion. Since instability occurs when the real part of a root becomes positive, plots of the root loci are useful in assessing the relative stability of various configurations under different towing conditions. Although the preceding mathematical model and solution are simple, computer simulations have shown good agreement with actual towing trials.

Parent System and Variations

The parent body used for analysis is a simplified model of DREA's Moby II[8] shown in Fig. 2. It is designed to achieve 250-ft depth at 40 knots with a limiting steady cable tension of 25,000 lb. The housing comprises halves of an 8.0-ft-long, 2.0-ft-diam body of revolution, separated by a 2.0-ft-deep prismatic section. It weighs 3000 lb in water and 5000 lb in air when fully flooded. Body centers of gravity, buoyancy, and housing hydrodynamic center are assumed coincident and located 1.0 ft vertically beneath the towpoint. This distance is the "housing lever" z_G. The depressing wing is designed to achieve a total downforce of 12,000 lb at 40 knots. Its L/V^2 is 2.0 lb-sec^2/ft^2 and its area is 8.0 ft^2. Wing hydrodynamic center coincides with the towpoint. The parent cable has a normal drag coefficient of 0.2 based on a 0.75-in.-diam and a friction ratio of 0.75. Standard towing conditions are 400 ft of immersed cable and 40 knots.

The parent body is referred to as the *depressed body*. When the wing is removed, the *wingless body* is obtained. The hypothetical *weight body* is an idealized high-density weight with negligible olume and hydrodynamic form, but is assumed to have the same drag as the wingless body.

Weights (for the weight body) of 3000 and 12,000 lb are used for comparison with the wingless and depressed bodies, respectively. Steady-state cable configurations with those body downforces at 40 knots are compared in Fig. 3. Note particularly the large increase in depression angle with increased downforce.

Root-Locus Plots

Figures 4–10 present the significant results of the parametric study in root-locus form. In these complex plane plots, the imaginary part of the characteristic equation root is the ordinate and the abscissa is the real part.

Characteristics of the parent depressed body at its design speed of 40 knots with 400 ft of cable are shown in Fig. 4. Longitudinal behavior consists of one lightly damped, long period oscillation; a heavily damped mode; and a pair of real roots indicating an overdamped mode. Lateral motion comprises a lightly damped, low-frequency "kiting" oscillation; a lightly damped "roll-yaw" coupled mode; and a heavily damped mode. The three lightly damped oscillatory

modes are most likely to be of practical interest. None of the three heavily damped modes displays important trends over the range of variations appropriate to statically stable bodies.

Longitudinal Subsidences

The longitudinal pair of real roots is strongly affected by pitch stiffness and surge damping. As indicated by the horizontal tail area and tail length trends in Figs. 5a and 5b, the smaller real root becomes positive when the body becomes statically unstable. It also approaches the origin as cable length is increased (Fig. 5e). This is caused by the decreased depression angle, which reduces cable surge damping. Inclusion of cable damping terms in the mathematical model is important to the simulation of this mode. Without cable damping, a very lightly damped, long period oscillation results—a type not observed in actual towing trials. The larger root is more sensitive but remains stable in all of the cases studied. It is most sensitive to a large change in wing lift at constant downforce, which is essentially a variation of pitch stiffness.

Figure 5 refers only to the depressed body. Analysis of weight bodies has shown that the smaller root approaches the origin as body drag, and consequently body surge damping, is reduced. However, depressed body or wingless bodies become unstable in this mode only when statically unstable.

An approximation for the smaller root may be derived from pitch and surge equations:

$$-\zeta\omega_n = -\tfrac{1}{2}\,[M_\theta X_{\dot{x}}/(M_\theta m + M_{\dot{\theta}} X_{\dot{x}})] \qquad (10)$$

It demonstrates the dependence of the root on pitch stiffness and surge damping, and facilitates understanding of tendencies exhibited in Fig. 5.

Long Period Longitudinal Mode

The most important oscillatory longitudinal mode is of low frequency (of order 0.5 rad/sec) and damping depends primarily on cable configuration parameters. It is mainly a heaving motion, although coupled significantly to pitch. Approximate equations for natural frequency and damping ratio may be derived from the heave and pitch equations:

$$\omega_n = [(Z_z/Z_{\dot{z}})\,(M_\theta/M_{\dot{\theta}})]^{1/2} \qquad (11)$$

$$\zeta = \frac{1}{2}\left[\left(\frac{M_\theta}{M_{\dot{\theta}}}\right)\left(\frac{Z_{\dot{z}}}{Z_z}\right)\right]^{1/2}\left[1 - \left(\frac{Z_\theta}{Z_{\dot{z}}}\right)\left(\frac{M_{\dot{z}}}{M_\theta}\right)\right] \qquad (12)$$

The influence of design features on this mode are shown in Fig. 6. Effect of varying tail length and area, and wing L/V^2 and area, are relatively slight (Figs. 6a and 6b).

The importance of depression angle in this mode is well illustrated by the effect of downforce, particularly in the case of the hypothetical weight bodies in Fig. 6c. These show a rapid decrease of damping as downforce increases, with negligible change in natural frequency. Cable heave spring constant increases at the same rate as body mass, hence, natural frequency remains constant. With frequency constant, damping ratio is proportional to the ratio of heave damping to body mass. Since cable heave damping increases much more slowly than the mass, damping ratio decreases.

Damping increases rapidly with cable drag for ballasted bodies at low depression angles. Figure 6c shows that very heavily ballasted bodies may encounter inadequate damping when towed with very low-drag cables. This figure and Fig. 6d show that the depressed body has a much lower natural frequency than weight or wingless bodies. The difference is due to a large reduction in cable heave spring constant at the lower depression angle, as well as larger virtual mass of the depressed body in heave.

Damping increases rapidly with cable length, going supercritical by 600 ft in the case of the wingless body and the 3000-lb weight. Conversely, in the case of the depressed body and the 12,000-lb weight, damping becomes unsatisfactorily light at short cable lengths. Cable length has a comparatively minor effect on the undamped natural frequency.

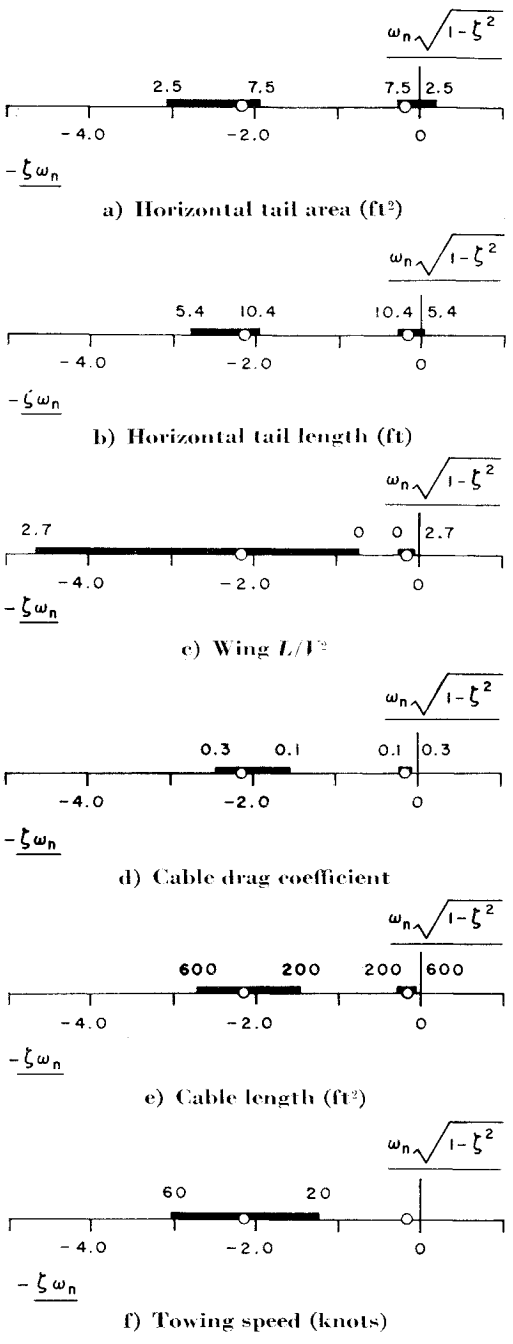

Fig. 5 Longitudinal subsidences—depressed body.

The effect of speed differs radically for the depressed and wingless bodies. With the wingless body, damping increases rapidly with speed, becoming supercritical by 60 knots, while there is little change in natural frequency. With the depressed body, however, the primary effect is an increase of frequency with speed, while damping actually decreases slightly. This difference is mainly due to the angle of depression of the cable which, for the wingless body, decreases much more rapidly with speed.

Heavily Damped Longitudinal Mode

The second longitudinal oscillatory mode has a high frequency (of order 5 rad/sec damped) and is well damped. It is not influenced by cable characteristics and is essentially a

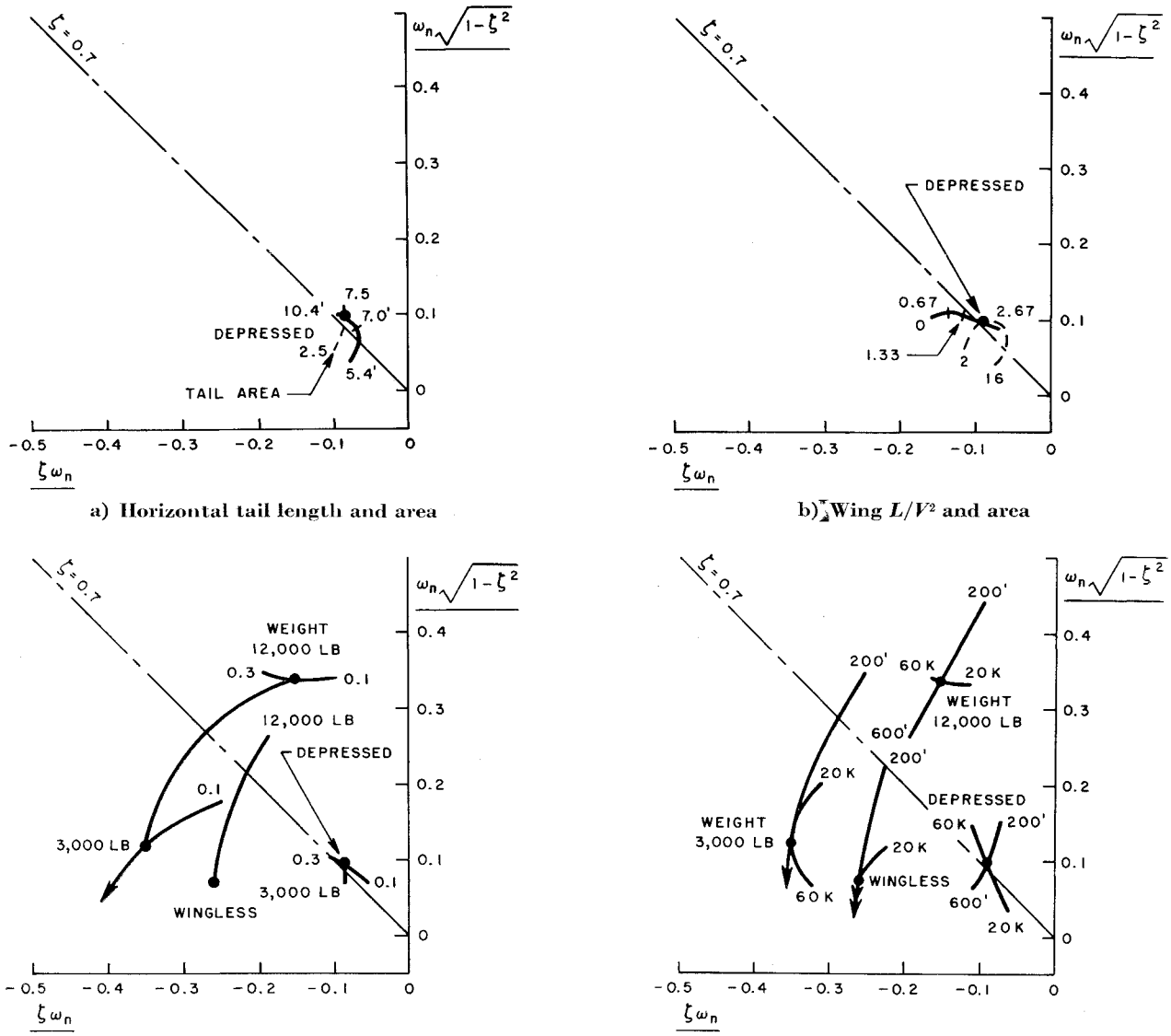

a) Horizontal tail length and area

b) Wing L/V^2 and area

c) Downforce and cable drag

d) Speed and cable length

Fig. 6 Long period longitudinal mode.

body pitch mode, although coupled to heave. For this reason, trends in this mode can be explained largely by the single degree-of-freedom pitch equation, which gives

$$\omega_n = (M_\theta/I_y)^{1/2} \tag{13}$$

$$\zeta = M_{\dot\theta}/2\omega_n I_y \tag{14}$$

where I_y includes virtual inertia in pitch.

Figure 7a shows that the primary effect of increasing horizontal tail length and area on this mode is a moderate increase in natural frequency consistent with the increased pitch spring constant M_θ. When the proportion of the downforce taken by the wing is varied, as in Fig. 7b, both frequency and damping are influenced by heave cross coupling. Increased heave damping due to increased wing area (or the addition of a wing to the wingless body) shown in Figs. 7b and 7c results in a large increase in damping ratio. Since damping is close to critical for all values of L/V^2 and wing areas, these effects are unlikely to have practical significance. Cable length has no effect on this mode.

As indicated in Fig. 7d, damping ratio is unaffected by speed, but natural frequency is strongly speed dependent, particularly when the wing is used. In fact, natural frequency increases roughly linearly with speed. Referring to Eq. (11) for natural frequency in two-degree-freedom motion in heave and pitch, Z_z and M_θ increases more rapidly with speed than do $Z_{\dot z}$ and $M_{\dot\theta}$.

Heavily Damped Lateral Mode

This is one of three lateral modes, all of which are oscillatory. It has a high frequency (of order 5 rad/sec, damped) and is nearly critically damped. It is not influenced by cable length and essentially involves body yaw about the towpoint with slight roll and sway coupling. Trends can be understood from the single degree-of-freedom yaw equations:

$$\omega_n = (N_\psi/I_z)^{1/2} \tag{15}$$

$$\zeta = N_{\dot\psi}/2\omega_n I_z \tag{16}$$

where I_z includes virtual inertia in yaw.

Figure 8 demonstrates that towing speed has by far the largest effect on natural frequency in this mode. In fact, the natural frequency increases roughly linearly with speed. Since N_ψ increases as speed squared, Eq. (15) shows this tendency. Figures 8a–8d show that damping ratio is affected by vertical tail length, height, and area, and by housing lever. None of these variations is significant, being confined to the region of near critical damping.

Roll-Yaw Coupled Mode

A second oscillatory lateral mode has an intermediate frequency (of order 1 rad/sec) and is a coupled roll-yaw motion, somewhat analagous to the "Dutch Roll" of an aircraft. Approximate expressions for natural frequency and damping ratio in two-degree-of-freedom roll and yaw motion are useful in understanding tendencies in this mode:

$$\omega_n = [K_\varphi N_\psi / (K_\varphi N_{\dot\psi} + N_\psi I_x)]^{1/2} \quad (17)$$

$$\zeta = (N_\psi K_{\dot\varphi} - N_{\dot\varphi} K_\psi + N_{\dot\psi} K_\varphi)/2\omega_n I_x I_z \quad (18)$$

Figure 9a shows instabilities in this mode when the depressed body has insufficient vertical tail length or area. Both natural frequency and damping ratio increase as vertical tail length and area increase. Roll coupling is not significant, and can be explained by simple yaw considerations.

Figure 9b shows housing lever to have an important effect on the coupled roll-yaw mode. From the zero value appropriate to a body of revolution, up to the design value, the change is essentially one of decreasing natural frequency; but beyond the design value, damping ratio increases because of the dominant effect of increased roll damping $K_{\dot\varphi}$. The trend for vertical tail height variation is very similar to that for housing lever at positive values. Increasing negative values cause an increase in damping ratio for the depressed body.

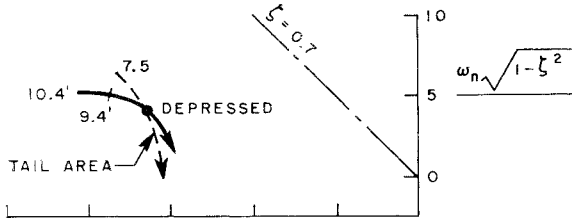

a) Horizontal tail length and area

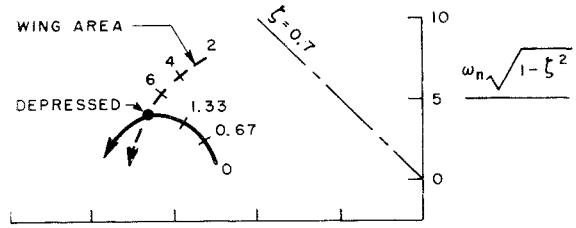

b) Wing L/V^2 and area

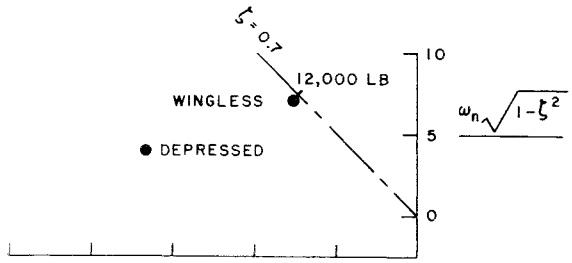

c) Downforce and cable drag

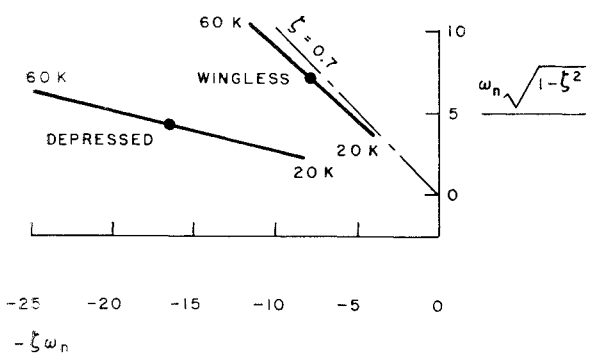

d) Speed and cable length

Fig. 7 Heavily damped longitudinal mode.

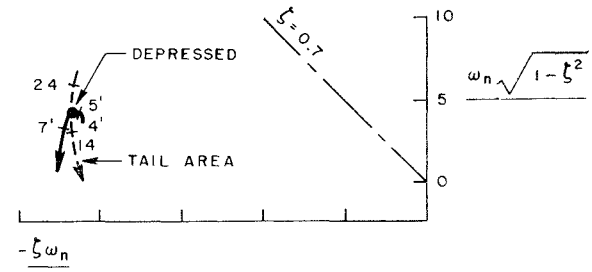

a) Vertical tail length and area

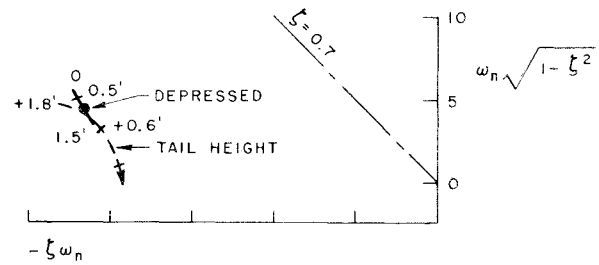

b) Vertical tail height and housing lever

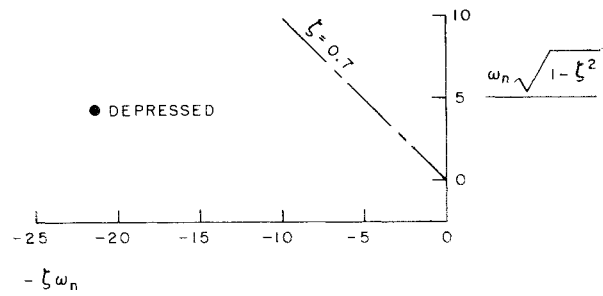

c) Wing L/V^2 and area

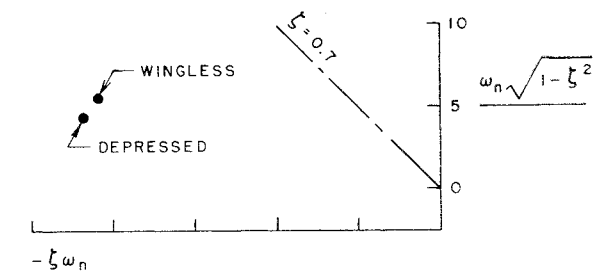

d) Downforce and cable drag

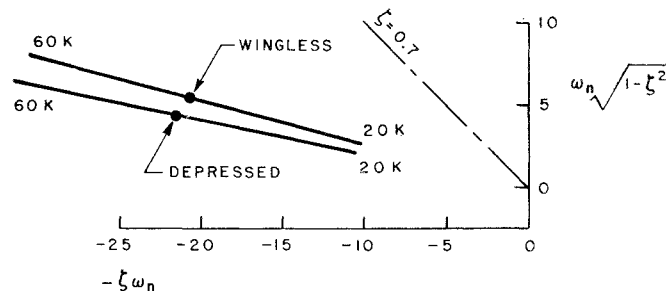

e) Speed and cable length

Fig. 8 Heavily damped lateral mode.

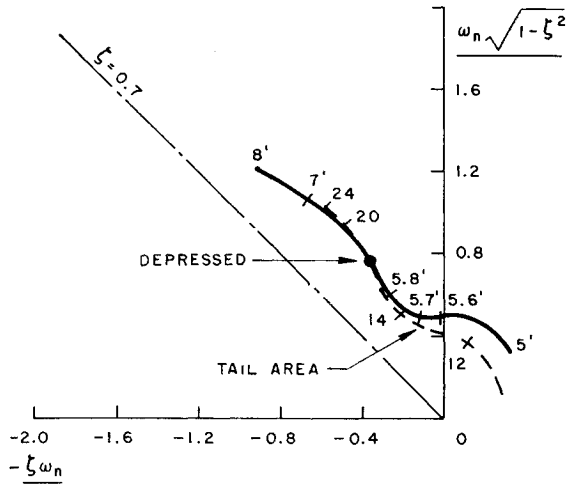

a) Vertical tail length and area

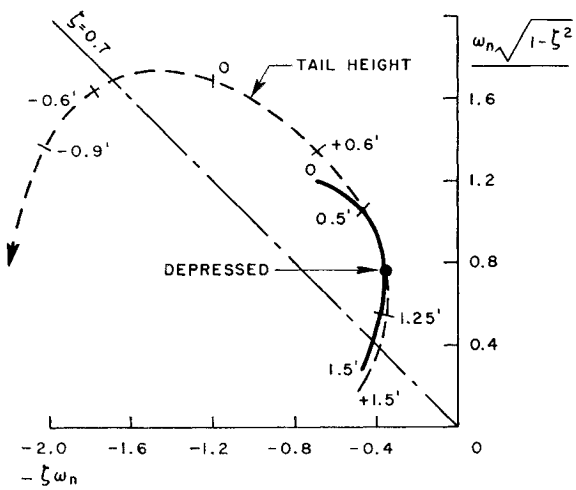

b) Vertical tail height and housing lever

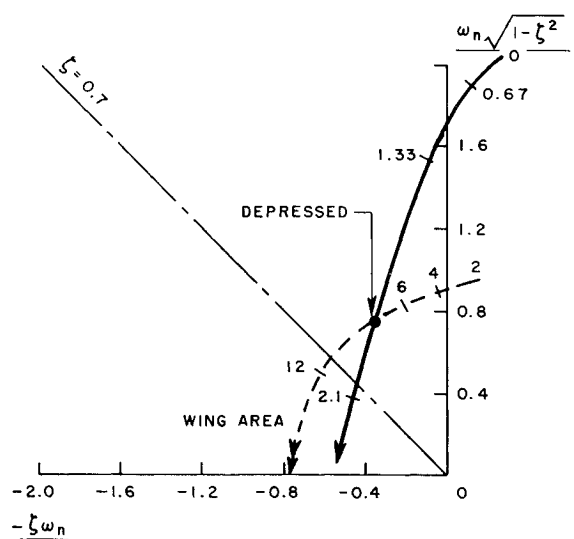

c) Wing L/V^2 and area

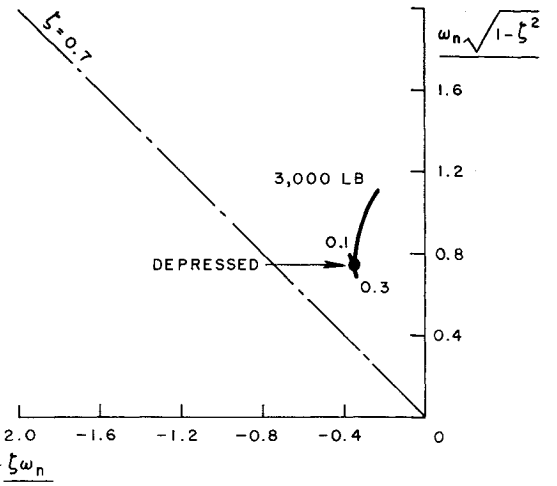

d) Downforce and cable drag

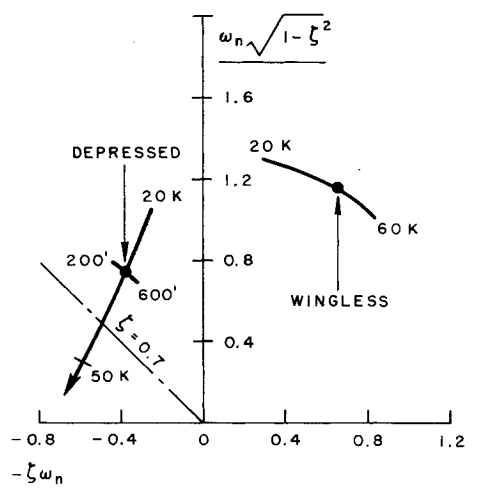

e) Speed and cable length

Fig. 9 Roll yaw mode.

The proportion of downforce taken by the wing and wing area have a very great effect on mode damping, as illustrated in Fig. 9c. Indeed, damping changes from negative values below an L/V^2 of about 1.0 or $S = 3.5$ ft^2 to supercritical values at an L/V^2 of about 2.2 or $S = 15$ ft^2. As L/V^2 is decreased, the corresponding addition of weight causes increased rolling moment due to roll K_φ which results in increased natural frequency and decreased damping ratio. Increased wing area results only in increased roll damping K_φ; hence, mode damping ratio is increased while natural frequency is unaffected.

Figure 9d shows that cable drag coefficient has little influence on roll-yaw coupled mode characteristics. Since cable parameters do not affect moments at the body towpoint, this is not surprising. On the other hand, reduction of downforce from 12,000 to 3000 lb causes an important decrease in damping and an increase in frequency. This is caused by reduced sway damping due to reduced depression angle. Therefore, sway coupling can be important for depressed bodies in this mode.

The wingless body exhibits instability in this mode at all speeds, as illustrated in Fig. 9e. When a hypothetical skeg is added to increase the roll damping, the effect is reversed and the locus becomes similar to that shown for the depressed body whose wing provides the necessary roll damping.

The damping ratio for the depressed body increases rapidly with speed, becoming supercritical by 60 knots. Natural frequency decreases slightly with speed. Referring to Eq. (17), speed has no effect on roll stiffness K_φ, whereas static directional stability N_ψ and the product of roll and yaw damping are proportional to speed squared—hence, frequency is relatively insensitive to speed. In Eq. (18) the dominant numerator product $N_\psi K_\varphi$ increases as speed cubed, while the denominator decreases slightly. Therefore, damping ratio increases rapidly with speed. Cable length has negligible effect on this mode.

Lateral Kiting Mode

The third lateral mode is a damped oscillation with a low frequency (of order 0.5 rad/sec) and relatively light and variable damping. This is primarily a swaying motion, although roll and yaw coupling can be important: pendulous kiting is perhaps an apt description.

Comparison of Figs. 9a and 10a show that the effect of vertical tail length or area on this mode is almost opposite to the effect on the coupled roll-yaw mode. At small tail lengths or areas, damping decreases rapidly with increasing tail length or area, but beyond 5.7 ft or 14 ft^2, a minimum value is reached, and it is then natural frequency that decreases with increasing tail length or area. These design features primarily affect yawing moment. The coupled sway and yaw equations given below help to illustrate the importance of their interaction:

$$\omega_n = [(Y_v/Y_{\dot{v}})(N_\psi/N_{\dot{\psi}})]^{1/2} \tag{19}$$

$$\zeta = (Y_v N_{\dot{\psi}} - Y_{\dot{\psi}} N_v)/2\omega_n Y_{\dot{v}} N_{\dot{\psi}} \tag{20}$$

Figure 10b shows that housing lever has an important effect on the damping of the long kiting mode, which decreases continuously with increasing housing lever and goes unstable by 1.5 ft. The effect on natural frequency is secondary. Again, it is notable that the effects on this and the roll-yaw mode tend to be opposite, requiring careful study and compromise in practical design. The effect of vertical tail height is similar except for an initial increase in frequency with little change in damping ratio for positive values.

Housing lever and vertical tail height primarily affect rolling moment, and the coupled sway and roll equations illustrate some of the important effects:

$$\omega_n = [Y_v K_\varphi/(Y_{\dot{v}} K_{\dot{\varphi}} - Y_{\dot{\varphi}} K_{\dot{v}})]^{1/2} \tag{21}$$

$$\zeta = (Y_{\dot{v}} K_\varphi + Y_v K_{\dot{\varphi}} - Y_\varphi K_{\dot{v}})/2\omega_n m_y I_x \tag{22}$$

Increased vertical tail height and housing lever result in increased $Y_{\dot{\varphi}}$ and $K_{\dot{v}}$ derivatives as well as increased moment of inertia I_x. Equations (21) and (22) show that these effects tend to increase natural frequency and reduce damping ratio as demonstrated in Fig. 10b.

Figure 10c shows that the effect of L/V^2 in this mode is again opposite to its effect on the roll-yaw mode. Up to the design value an increasing natural frequency is the primary effect. Beyond the design value, the curve turns over rapidly and damping ratio drops off quickly, producing instability beyond an L/V^2 of about 2.15. Equation (21) shows that the reduction in ω_n with increased L/V^2 can be explained by a reduction in roll stiffness due to the reduction in weight needed to maintain constant downforce. Equation (22) demonstrates that damping ratio is strongly affected by the weight decrease associated with L/V^2 since not only K_φ in the numerator decreases but ω_n, m_y, and I_x in the denominator are also affected. Increased wing area results in increased roll damping, which in turn reduces the natural frequency according to Eq. (21). The effect on natural frequency, rather than the product $Y_v K_{\dot{\varphi}}$, dominates the root locus trend, according to Eq. (22).

Figure 10d indicates that the major effect of increased cable drag coefficient is to increase the natural frequency of this mode. Such results are consistent with the effect of reduced depression angle upon cable spring and damping terms.

Comparison of the effects on natural frequency of increased downforce on the weight body and the depressed body shows opposite trends. For the weight body, a decrease of natural frequency with mass is the dominant effect. In the case of the depressed body there is no change in mass, since the additional downforce is achieved with wing lift alone. The increased cable spring constant and increased sway-roll coupling are the important effects.

Figure 10e shows that the primary effect of cable length is on damping, which becomes unsatisfactorily light at short cable lengths, particularly for the depressed body. There is a secondary effect on the undamped natural frequency, which decreases with increasing cable length. These trends are consistent with changes in cable spring and damping with cable length, and with increased sensitivity to cable length at high depression angles.

For realistic bodies, speed primarily increases natural frequency. However, for the depressed body, beyond 40 knots there is an increasingly rapid deterioration of damping and the mode goes unstable at about 50 knots. This is mainly the effect of the unfavourable sway-roll coupling term Y_φ in Eq. (22). The value of Y_φ reflects the fact that wing lift rolls with the body, and this lift dominates the downforce at high speeds. In this mode, it is this effect that is most likely to impose a limit on towing speeds in practice, without using automatic controls.

Concluding Remarks

A simple linear mathematical model has validity and utility in the analysis of cable-towed body system design features and dynamic stabilities. Some of the six fundamental modes of motion are quite complex, despite the modeling method and the simple parent study configurations used. Nevertheless, useful design information has been generated as root-locus plots. These indicate the relative significance of the 6 modes, approximate equations for mode trends, and relative importance of body design and cable configuration effects in each mode. Of the six modes of motion exhibited, three are likely to be significant and three insignificant for statically stable depressed bodies of the type studied.

The three insignificant modes are as follows:

1) The heavily damped longitudinal mode is a body-dominated pitching oscillation, with undamped natural frequency varying linearly with speed.

2) The heavily damped lateral mode is a body-dominated yawing oscillation, with undamped natural frequency varying linearly with speed.

3) The longitudinal subsidence mode is a nonoscillatory mode, which is stable unless the body is statically unstable.

The three modes likely to be significant are as follows:

1) The long period longitudinal mode is a towing configuration mode affected little by body design details. This is a low frequency, variably damped heaving oscillation, with strong pitch coupling effects. Its damping is sensitive to cable length and other parameters affecting system depression angle. Heavily ballasted bodies towed at low speeds on low drag cables may go unstable at very short cable lengths.

2) The coupled roll-yaw mode is the most sensitive body design mode and is affected little by cable configuration variables. This is an intermediate frequency and damping, coupled rolling, and yawing oscillation, similar to aircraft Dutch roll. Bodies with low roll damping have shown instabilities in this mode in actual towing trials. Inadequate vertical tail length or area results in instability.

3) The lateral kiting mode is sensitive to both towing configuration and body design variables. This is a low frequency, lightly damped swaying or kiting oscillation with important roll and yaw coupling effects. Its damping is sensitive to cable length and to wing and vertical surface

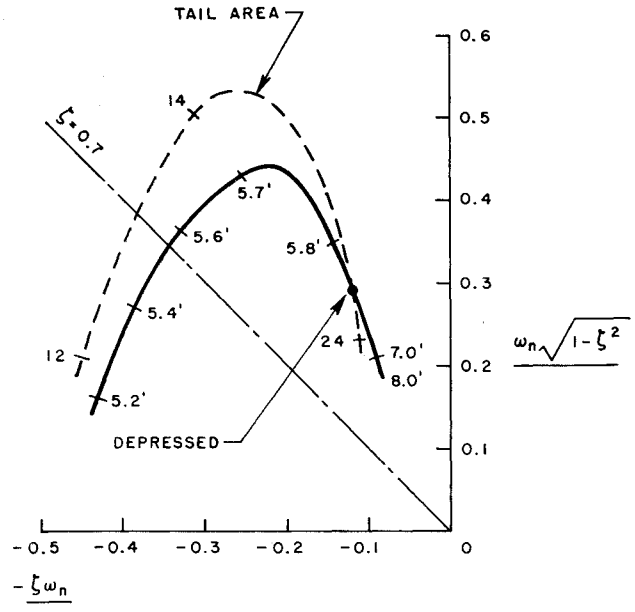

a) Vertical tail length and area

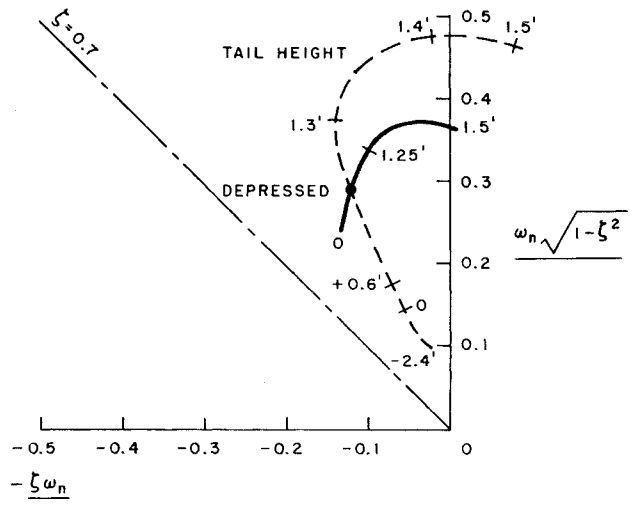

b) Vertical tail height and housing lever

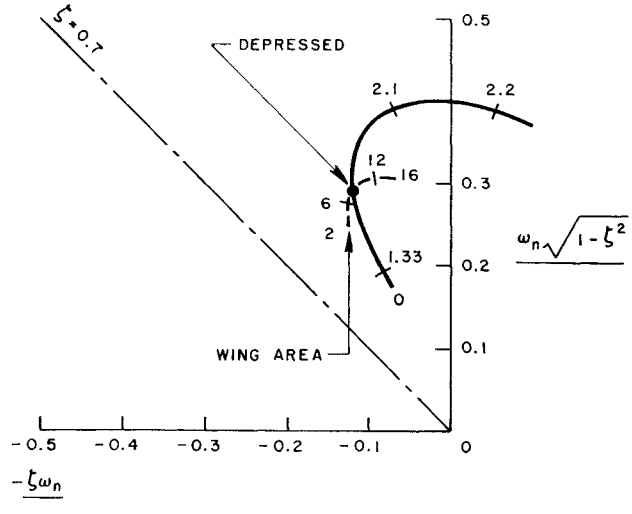

c) Wing L/V^2 and area

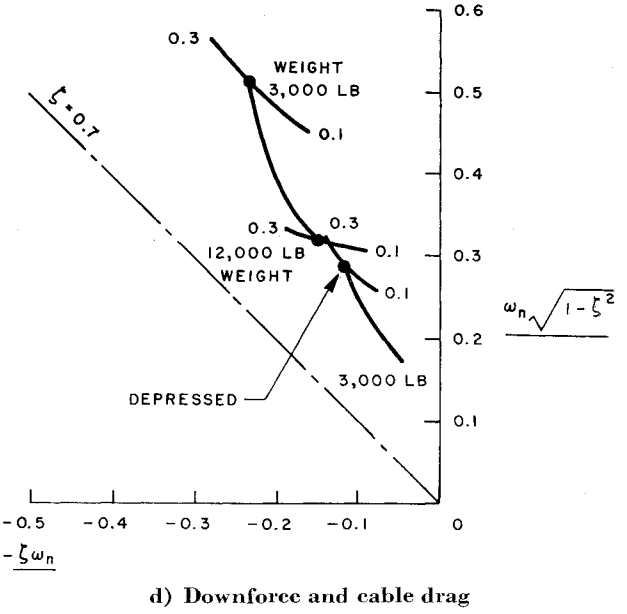

d) Downforce and cable drag

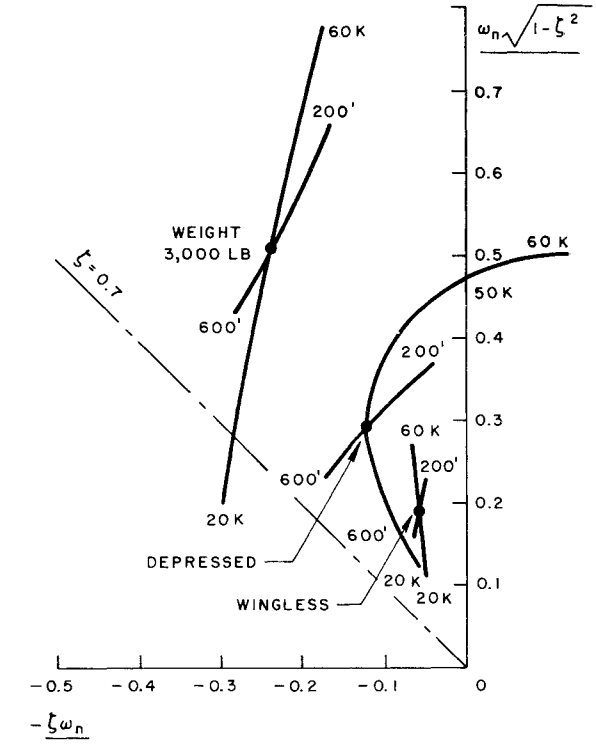

e) Speed and cable length

Fig. 10 Lateral kiting mode.

parameters. In particular, large wing lift (in relation to ballast) can cause instability in this mode, as can excessive vertical surfaces.

It is particularly important to note that body design variables tend to produce significant opposing effects in the lateral kiting and coupled roll-yaw mode. The system designer must be aware of these tendencies, since they demand careful compromise.

References

[1] Eames, M. C., "Steady-State Theory of Towing Cables," *Quarterly Transactions RINA*, Vol. 110, No. 2, April 1968.

[2] Whicker, L. F., "The Oscillatory Motion of Cable-Towed Bodies," Doctoral thesis, May 1957, Univ. of California, Berkeley, Calif.

[3] Lum, S. M. Y., "A Theoretical Investigation of the Body Parameters Affecting the Open-Loop Pitch Response of a Submerged Towed Body," Rept. 1369, Feb. 1960, David Taylor Model Basin, Carderock, Md.

[4] Strandhagen, A. G. and Thomas, C. F., "Dynamics of Towed Underwater Vehicles," Research Rept. 219, Nov. 1963, U. S. Navy Mine Defense Lab., Panama City, Fla.

[5] Richardson, J. R., "The Dynamics of Towed Underwater Systems, Part I. Stability of the System," Rept. 56, 1965, Engineering Research Associates, Toronto, Canada.

[6] Patton, K. J. and Schram, J. W., "Equations of Motion for a Towed Body Moving in a Vertical Plane," Rept. 736, June 1966, U.S. Navy Underwater Sound Lab., New London, Conn.

[7] Laitinen, P. O., "Cable-Towed Underwater Body Designs," Rept. 1452, April 1967, U.S. Naval Electronics Lab., San Diego, Calif.

[8] Eames, M. C., "Experimental Bodies for High-Speed Underwater Towing Research," *Canadian Aeronautics and Space Journal*, Vol. 13, No. 5, May 1967.

OCTOBER 1968 J. HYDRONAUTICS VOL. 2, NO. 4

A Three-Dimensional Dynamic Analysis of a Towed System

JEFFREY W. SCHRAM*
Newark College of Engineering, Newark, N.J.
AND
STANLEY P. REYLE†
Rutgers University, New Brunswick, N.J.

The purpose of this investigation is to study the three-dimensional motion of a cable-body towing system. By assuming that the towline is continuous, completely flexible, and inextensible, three first-order partial differential equations of motion are developed in terms of velocity components normal and tangential to the towline. In addition to these, three kinematical first-order partial differential equations are generated to describe the position of the towline in space. The boundary conditions for the system are the motion of the towing ship and the forces exerted by the towed body. The dynamic motion of the towed system is obtained by applying the method of characteristics to the equations of motion. The characteristic equations are then numerically integrated on a computer. A transfer function, which is defined as the ratio of the resultant body amplitude of motion to the amplitude of the ship motion, is developed for various towing speeds and towline lengths. The transfer function decreases as the towline length and the towing speed increase for the examples given in this paper. Also, it is shown that, if the towline is not straight, then longitudinal disturbances produce transverse disturbances and vice versa.

Nomenclature

A_B	=	plan area of the towed body
A_C	=	cross-sectional area of towline cable
C	=	towline steady-state velocity with respect to the water
C_D	=	towline fairing drag coefficient
c	=	towline fairing chord
D_N	=	normal towline drag force per foot
E	=	Young's modulus for the towline
F	=	normal towline hydrodynamic force per foot $[(H^2 + I^2)^{1/2} = F = (D_N^2 + L^2)^{1/2}]$
F_B	=	hydrodynamic body force
$F_\alpha, F_\beta, G_\alpha, G_\beta$ $H_\alpha, H_\beta, L_\alpha, L_\beta$	=	defined by Eqs. (66-74)
I, G, H	=	hydrodynamic towline forces in the x, y, z direction, respectively
L	=	towline lift force per foot
L_C	=	total length of towline
M_B	=	mass of body
R	=	$(U^2 + W^2)^{1/2}$
R_e	=	Reynolds number
R_d	=	$\rho/2cC_DR^2$
s	=	arc length along towline
t	=	time
U, V, W	=	velocity components in the x, y, z direction, respectively
u, v, w	=	velocity components in the X, Y, Z direction, respectively
VOW	=	$V_0 \cos\theta_0 - W_0 \sin\theta_0$
W_B	=	weight of body in water
W_l	=	weight of towline per foot in water
X, Y, Z	=	spatial coordinates of the towline
x, y, z	=	coordinates aligned with the towline
δ	=	boundary-layer thickness
δK	=	time increment for numerical solution
δh	=	arc length increment for numerical solution
ϕ, θ	=	directional angles of the towline
ρ	=	density of fluid
μ	=	mass of towline per foot
μ_f	=	viscosity of fluid

Subscripts

d	=	dynamic properties
L	=	boundary condition at the body
T	=	directed along the towline
u	=	condition at the surface
0	=	steady-state condition
1	=	small perturbation about a steady-state value
α	=	directed along the α characteristic line

Received May 16, 1968. The authors wish to thank the U.S. Navy Underwater Sound Laboratory and especially S. Gross and K. Patton for supporting the project that produced this paper.

* Assistant Professor, Department of Mechanical Engineering.

† Associate Professor, Department of Mechanical Engineering. Member AIAA.